Robust RFID-based Respiration Monitoring in Dynamic Environments

Yanni Yang, Jiannong Cao

Department of Computing, The Hong Kong Polytechnic University, Hong Kong, China.

yan-ni.yang@connect.polyu.hk, jiannong.cao@polyu.edu.hk

Abstract—**Respiration monitoring (RM) is essential for diagnosing and tracking respiratory diseases. Recently, RFID technology has enabled RM in a lightweight and cost-effective way by only attaching the tiny and cheap RFID tag on the monitored person's chest. However, current systems are mostly designed for static environments with no surrounding people's movements. In reality, dynamic environments where people could move nearby the monitored person are quite common. In such environments, respiration signals would be disturbed by the dynamic multipath signals from ambient movements, which may lead to inaccurate RM results. In this paper, we study how to realize robust RFID-based RM in dynamic environments with accurate respiration rate estimation and apnea detection. We find that the dynamic multipath signals can cause not only high-frequency noises but also fake and distorted respiration cycles, which cannot be simply removed by the low-pass filter. Thus, we need a new method to eliminate the effect of multipath signals. Inspired by the intrinsic features of human respiration pattern, we propose to transform the respiration pattern into a matched filter, which can extract the real respiration cycles out of noisy RFID signals. We then estimate the respiration rate by counting the respiration cycles via multi-scale peak detection. For apnea detection, the problem from multipath signals is that the fake respiration cycles can result in the missing detection of apnea when the monitored person stops breathing. To address this issue, we define a new indicator which measures the dominance of respiration components in the signal's spectrum to identify apnea from multipath signals. Experimental results show that our system achieves an average error of $0.5\ bpm$ for respiration rate estimation and a 5.3% error for apnea detection in dynamic environments.**

Index Terms—**Respiration monitoring, RFID, Multipath effect**

I. INTRODUCTION

Respiration state is an important metric to observe and monitor people's health conditions. Many respiratory diseases, *e.g.*, sleep apnea [1], asthma, and chronic obstructive pulmonary disease (COPD) [2], can be reflected from the respiration state. Thereby, respiration monitoring (RM) is highly required for people suffering from respiration disorders.

Traditional RM systems are cumbersome. People need to wear tight devices on the body, *e.g.*, the chest belt and nostril sensor. These devices could make people feel uncomfortable, especially during sleep. Recently, radio frequency (RF) signals have shown their capability for non-intrusive RM, which aims to release people from bulky sensors [3]–[9]. Among RF signals, RFID signals have been widely exploited for RM [10]–[12]. By attaching the RFID tag on the monitored person's chest, tag signals can capture the periodic respiration pattern while breathing. RFID signals have many advantages over other RF signals for RM. Compared with WiFi signals which have limited usage for multi-person RM [5] [3], RFID tags can be attached on different persons' chests to simultaneously and separately monitor their respiration. Compared with radar signals, *e.g.*, FMCW [8] [9], which requires dedicated devices, RFID devices are widely available in the market, and the cheap RFID tags make it more cost-effective.

However, current RFID-based RM systems can only work when the monitored person is in a static environment where no people move around, so that respiration is the only motion [10]–[13]. While dynamic environments with surrounding people's movements are quite common in many RM scenarios. For instance, if a person is watching TV in the living room with RM running at the same time, family members could pass by from time to time. Hence, RM systems should also work properly in dynamic environments. However, the movements of surrounding people could bring dynamic multipath signals which are superimposed with the desired line-of-sight (LOS) respiration signals of the monitored person. Then, the respiration pattern in the RFID signals would be distorted, which may result in wrong RM results. Therefore, in this work, our goal is to remove the effect of multipath signals in dynamic environments for realizing robust RFID-based RM with accurate respiration rate estimation and apnea detection.

To achieve this goal, *the first task is to understand how the dynamic multipath signals of moving people affect the respiration signals of the monitored person.* Previous work models the effect of multipath signals on the RFID phase values in a general way [14] [15]. However, the change of RFID phase values incurred by multipath signals is subject to many factors, *e.g.*, antenna radiation range, people's moving area and pattern. Therefore, in our work, we perform a detailed investigation of these factors' effects on the RFID phase value changes. We find that the multipath signals of moving people can bring similar order of magnitude changes on the phase values compared with those resulting from the chest movement during respiration. In addition, the multipath signals could distort the original respiration signals with both high-frequency noises and fake respiration cycles, which could cause wrong respiration state measurements.

Thus, *the second task is to remove the multipath effect on respiration signals for accurate respiration rate estimation.* To achieve this, we get insights from the inherent features of the human respiration pattern. Human-beings have a stable and

periodic respiration rhythm which is unique and diverse among individuals [16]. Compared with the random ways of people's moving, respiration presents a regular and rhythmic pattern. This inspires us to transform a real respiration cycle into a matched filter to denoise the respiration signals mixed with multipath signals. Then, there will be peaks in the matched filter output which match the corresponding respiration cycles. By detecting the peaks, we can estimate the respiration rate accordingly. However, the performance of the matched filter depends on the shape of the respiration cycle. Since respiration patterns are diverse for different persons, a unique respiration cycle template should be created for each user to have their own matched filter. So, we propose a cycle-averaging method to generate the respiration cycle template beforehand.

The third task is to accurately detect the apnea, which is a symptom of sudden breathing stop. In dynamic environments, the ambient movements can result in the missing detection of apnea for the monitored person. This is because when the monitored person stops breathing with no respiration signals generated, the multipath signals may make the phase values change like the respiration pattern. This would leave a false impression that the person is still breathing and lead to the missing diagnosis of apnea. To address this issue, we observe the spectrum of respiration and multipath signals in the frequency domain and compare the dominance of their frequency components within the respiration rate range. For respiration signals, the most dominant frequency components fall into the respiration rate range. While the respiration frequency components of multipath signals take up only a small portion over the whole spectrum. Thus, we define a respiration-to-noise ratio (RNR) which measures the percentage of respiration components over all the frequency components in the spectrum. The measured RNR is compared with a pre-defined threshold to identify the apnea out of the multipath signals.

In summary, our work makes the following contributions:

- To the best of our knowledge, we are the first to study the problem of RFID-based RM in dynamic environments. We can accurately estimate the respiration state when people move in the vicinity of the monitored person.
- We perform detailed analyses on how multipath signals of ambient people's movements affect the respiration signals. We investigate the key factors that affect the magnitude and pattern of multipath signals, which promotes the understanding of RFID multipath effect in this field.
- Based on the intrinsic feature of respiration, the matched filter is applied to denoise signals for respiration rate estimation. Spectrum analysis is done to aid apnea detection. Experimental results show that our system achieves similar performance on respiration rate estimation (0.5 bpm error) and apnea detection (5.3% error) in dynamic environments compared with those for static environments.

II. UNDERSTANDING RFID-BASED RESPIRATION MONITORING AND THE MULTIPATH EFFECT

In this section, we will introduce the preliminaries of the RFID tag phase and analyze how the phase values are affected
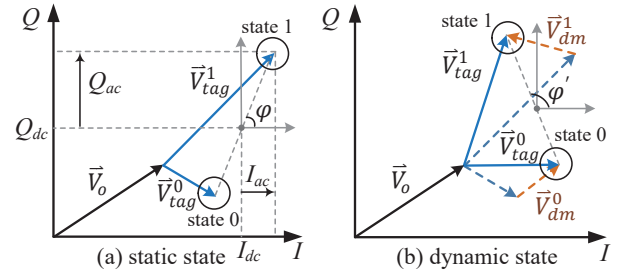

Fig. 1. Demodulated voltage of tag response received by the RFID reader

by both of the respiration activity and multipath signals.

A. Preliminary of RFID tag phase

The RFID antenna controlled by the reader sends out signals to interrogate the tag. After powering up the tag, the signals will be backscattered to the antenna. Then, the reader can capture the power and phase of tag signals. Here, the tag phase is used to measure the respiration state, since the phase value is more sensitive to the minute chest movement during breathing [10]. To interpret the tag phase, we refer to the phasor space, as shown in Fig. 1(a), to show how the phase is measured. The tag response received by the reader is transformed into a baseband signal $\vec{V}$, which can be represented as follows [17].

$$\vec{V} = \vec{V}_o + \vec{V}_{tag}^i; \ \vec{V}_o = \vec{V}_{leak} + \vec{V}_{scatter} \qquad (1)$$

$\vec{V}_o$ is decided by the reader transmitter to receiver leakage $\vec{V}_{leak}$ and scattering $\vec{V}_{scatter}$ from the environment. $\vec{V}_{tag}^i$ is the voltage of the tag backscattered signals of interest. $\vec{V}_{tag}^i$ changes with the state of the tag chip (i = state 0 or 1), which indicates the matching and mismatching state between the input impedance of the tag antenna and the tag chip [18]. The volume of $\vec{V}$ can affect the detection of the tag signals. If $\vec{V}$ becomes too small, $e.g.$, the tag is far from the reader, the tag will not be detected. After removing the DC component in $\vec{V}$, the phase ϕ is calculated as follows.

$$\phi = ang(\vec{V}_{tag}^1 - \vec{V}_{tag}^0) = arctan(\frac{Q_{ac}}{I_{ac}}) \qquad (2)$$

Q_{ac} and I_{ac} refer to the AC quadrature and in-phase components, respectively. When the tag moves, $\vec{V}_{tag}^1$ and $\vec{V}_{tag}^0$ rotate together and the phase value changes accordingly.

The magnitude of phase value can also be viewed from signal's travelling distance d, which is expressed as follows.

$$\phi = \{2\pi \cdot \frac{d}{\lambda}\} \mod 2\pi \qquad (3)$$

λ is the wavelength. For respiration monitoring, the tag is attached on the chest. When the chest expands and contracts, it brings $d_r(t)$ change to the tag displacement. If the tag faces to the antenna directly, Equ. (3) becomes the below expression.

$$\phi = \{2\pi \cdot \frac{2[d_0 + d_r(t)]}{\lambda}\} \mod 2\pi \qquad (4)$$

d_0 is the initial distance between the tag and the antenna. $d_r(t)$ is a sinusoidal function about the chest movement. It shows
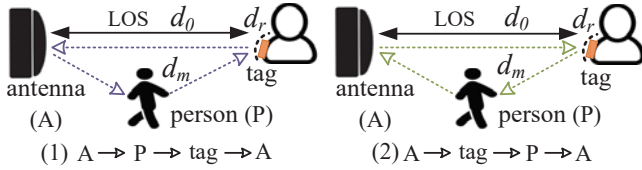
Fig. 2. Propagation path of multipath signals from moving person

(a) antenna radiation area   (b) setting of antenna & tag

Fig. 3. Illustration of RFID antenna radiation range and 3 dB beamwith

that phase values will change periodically with valleys and peaks indicating the expansion and contraction of the chest.

B. Tag phase of multipath signals

RFID-based RM systems are commonly designed to employ the LOS signals, which directly traverse between the antenna and tag, for respiration pattern extraction [10]–[12]. While there are many reflectors in the environment, *e.g.*, surrounding people and furniture. These reflectors bring multipath signals, which are superimposed with LOS signals. So, the $\vec{V}_m$ induced by multipath signals is added on $\vec{V}_{tag}$ in the I-Q plane. $\vec{V}_m$ involves static and dynamic components. Static components are those reflected by stationary objects (*e.g.*, desk and chair), which can be merged into $\vec{V}_o$. Dynamic components ($\vec{V}_{dm}^i$), as added in Fig. 1(b), come from moving objects, *e.g.*, people moving around. Meanwhile, multipath signals also add another component in the phase values with the travelling distance of $d_m(t)$, and Equ. (4) changes to the following expression.

$$\phi = \{2\pi \cdot \frac{2[d_0 + d_r(t)] + d_m(t)}{\lambda}\} \mod 2\pi \qquad (5)$$

In [14], it tells that dynamic multipath signals can make phase values change periodically within 2π with the object's moving. While the respiration chest displacement also leads to periodic phase changes within 2π [10]. Thereby, we need to compare the magnitude and pattern of the phase changes caused by the multipath signals with those from the respiration activity. Since multipath signals bring $\vec{V}_{dm}$ and $d_m(t)$ in phase values, we will next study how people's moving[1] affects these two variables regarding the phase value changes.

1) Effect of $\vec{V}_{dm}$: To investigate the effect of surrounding people's movements on $\vec{V}_{dm}$, we look into the propagation ways of multipath signals. As shown in Fig. 2, multipath signals propagates in two ways [14]: (1) antenna (A) → person (P) → tag → antenna; (2) antenna → tag → person → antenna.

In propagation way (1), the moving person affects the downlink of multipath signals, *i.e.*, [antenna → person → tag]. At this point, $\vec{V}_{dm}$ mainly depends on the person's reflection of the signals from the antenna to the tag. Suppose people reflect the same amount of signals, the key factor affecting $\vec{V}_{dm}$ is the person's moving area. For the directional RFID antenna, it has an effective radiation area, inside which a 3 dB beamwidth area (denoted as 3 dB-area) exits. Fig. 3(a) shows a 3 dB-area for a Laird antenna [19]. The area inside the red circle is the effective radiation range, and the inner area segmented by the

---

[1]Here, we mainly discuss the effect of walking movement because it is a common activity and involves larger body movements. We will investigate the effect of other movements in the evaluation section.
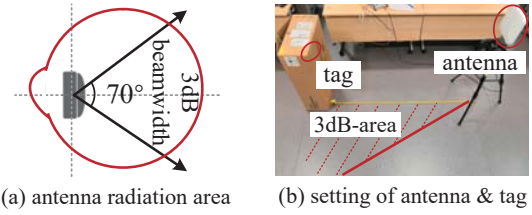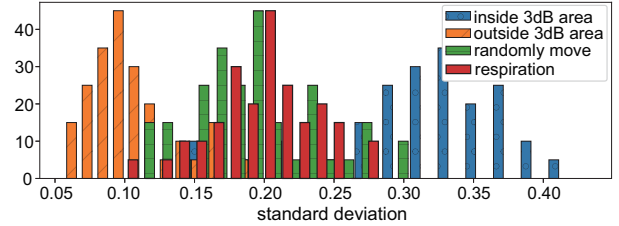

Fig. 4. Distribution of standard deviation of the phase value with moving people moving in different areas

two black arrows is the 3 dB-area. The signal power reduces by half and attenuates significantly outside the 3 dB-area [20]. If the person moves outside the 3 dB-area, the strength of the reflected signals becomes smaller or even equal to zero. Then, $\vec{V}_{dm}$ decreases, making the phase values change slightly.

To see the effect of people's moving area on phase changes, we attach a tag on a paper box and place the antenna 1.5 m away facing to the tag straightly, as shown in Fig. 3(b). A red line is drawn on the ground as the 3 dB beamwidth boundary. Volunteers are asked to walk inside, outside and randomly in and out of 3 dB-area without blocking the LOS path to generate multipath signals, respectively. The distributions of the standard deviation (std) of the phase values for people moving inside, outside and randomly in and out of 3 dB-area are shown in Fig. 4. We also depict the std of the phase values caused by the mere respiration activity for comparison. From Fig. 4, we can obtain the following observations: (1) The std distribution of the phase values when people move inside 3 dB-area is larger than that of outside 3 dB-area. This is because the movements inside 3 dB-area can result in larger $\vec{V}_{dm}$. (2) The std distributions of the random moving and respiration overlap a lot, showing that the multipath signals of moving people have similar effects on the phase changes compared with the respiration activity. Since the 3 dB-area is relatively small and people tend to walk arbitrarily inside and outside the area, people's moving could bring comparable phase changes as the respiration activity.

For propagation way (2), the moving person affects the uplink of multipath signals, *i.e.*, [tag → person → antenna]. In this case, $\vec{V}_{dm}$ is mainly decided by the person's reflection of the signals from the tag to the antenna. So, the distance between the person and tag matters for the phase changes. To see its effect, we ask a person to walk along a straight line with l distance to the antenna-tag yellow line under the setting in Fig. 3(b). The average std of phase values for different l is given in Fig. 5. The std falls sharply at the beginning. After
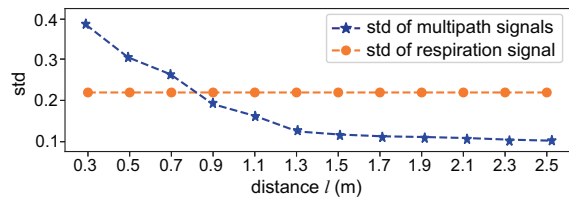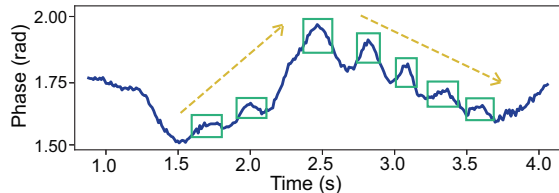
Fig. 5. Standard deviation of phase values for different distances l

Fig. 6. Phase values of the multipath signals caused by people walking around

Fig. 7. Multipath mixed respiration signals, ground truth respiration signals, and peak detection results

Fig. 8. Sketch of system overview

around $1\ m$, the std decreases smoothly and get close to 0. Compared with the mean std of respiration phase values (the straight line), multipath signals can be ignored when people are far from the monitored person. But, for people moving closely around the monitored person, multipath signals will affect the respiration pattern and should be removed.

2) Effect of $d_m(t)$: Next, we investigate the effect of people's moving pattern, *i.e.*, $d_m(t)$, on the phase values. People's moving routes can be random and unpredictable. Thus, it is difficult to describe $d_m(t)$ in a mathematical expression. But we can try to analyze the effect of $d_m(t)$ in another way. First, the overall increasing and decreasing trend of $d_m(t)$'s length can result in the general growth and decline of phase values. Second, the dynamic multipath signals bring constructive and destructive effects on the received signals, making the phase values change periodically [14]. The frequency of the periodic phase changes can be expressed as $f = 2v/\lambda$ [21]. v is the walking speed, which falls in the range of $0.5 - 1.5\ m/s$ [22]. Then, f is in the range of $3 - 9\ Hz$, which is much higher than the respiration rate range $0.17 - 0.5\ Hz$ [23]. In Fig. 6, we show the phase values of the multipath signals when a person walks by a static tag. The tiny and frequent peaks, highlighted with green rectangular, are due to the person's walking activity. Apart from the high-frequency peaks, there is also a general increasing and decreasing trend during $1.5\ s - 3.5\ s$, outlined with yellow arrows. This is owing to the change of the person's moving route, which makes the length of $d_m(t)$ to grow first and decline later. This general trend looks similar to the respiration pattern. Thus, the multipath signals also bring low-frequency components which can act as fake respiration cycles.

C. Respiration signals mixed with multipath signals

As discussed above, the multipath signals of moving people could distort the respiration signals with comparable magnitude changes of phase values, which carry both high-frequency noises and fake respiration cycles. Here, we attach an RFID tag on a person's chest and ask another 2 persons to walk around to show the respiration phase values mixed multipath signals in Fig. 7(a). Meanwhile, the ground truth signals of respiration
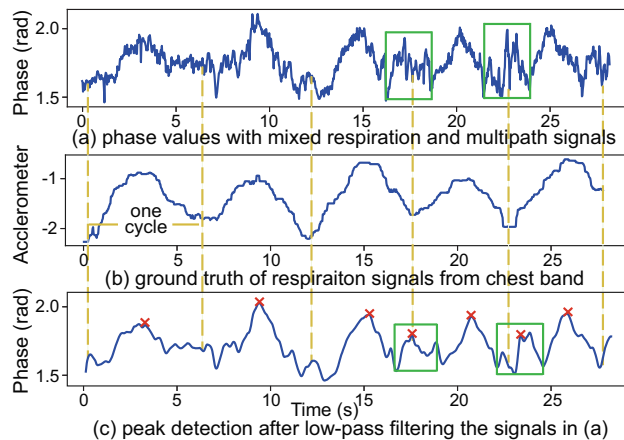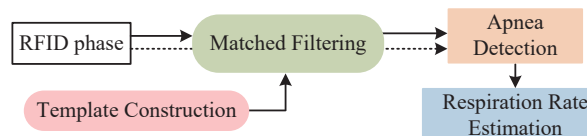
are collected with a chest band and shown in Fig. 7(b). The person breathes 5 respiration cycles. But, it is not clear to see the exact respiration cycles in the raw phase values which are messed up with high-frequency and low-frequency noises. In particular, the first respiration peak is quite flat and low. The peaks in the green rectangular, which are not respiration cycles, look similar to the respiration peaks. If we apply peak detection directly on the phase values after low-pass filtering [5], as shown in Fig. 7(c), 7 respiration cycles are detected. Then, the respiration rate will be wrongly estimated. Besides, the multipath signals also result in wrong apnea detection. In static environments, the phase values would keep stable during apnea. We can detect the apnea by observing whether phase values are above a certain threshold. However, if people are moving around the monitored person, multipath signals will incur the phase values to change, which could cheat the apnea detection algorithm that the person is still breathing.

III. OUR APPROACH

In this section, we will introduce how we eliminate the multipath effect in dynamic environments for accurate respiration monitoring. We will first present the overview of our approach and then go into the details of each module.

A. Overview

The system overview is depicted in Fig. 8. The raw RFID phase values are first collected from the tag and segmented into fix-length windows.[2] Then, the matched filter is employed to denoise the respiration signals mixed with multipath signals. The matched filter is created with the respiration cycle

---

[2]We perform RM only when the user is quasi-static without major movements. The method in [5] is used to detect whether the user moves.

template generated in the template construction module. As template shape can influence the performance of the matched filter, we pre-collect the phase values when the monitored person breathes in a static environment to construct a unique template. Then, the original phase values together with the matched filter output are passed to the apnea detection and respiration rate estimation modules. Apnea detection is done by transforming the phase values in a window into the frequency-domain spectrum and judging the dominance of the respiration rate components. The matched filter output of those windows without apnea will be processed to estimate the respiration rate by detecting the peaks in the matched filter output.

Fig. 9. Phase values of two persons' respiration activity

Fig. 10. Matched filter output of the signals in Fig. 7(b)

B. Matched filtering

To obtain the real respiration pattern from the noisy multi-path signals, an intuitive way is to apply the low-pass filter to remove the high-frequency components in the phase values. But the peak detection results in the last section has shown that it does not work well because the multipath signals also bring low-frequency components, which result in fake respiration cycles. To tackle this issue, we leverage the intrinsic differences between the pattern of respiration and multipath signals. Respiration signals are regular and sinusoidal with a known pattern. Multipath signals are more like random noises, which involve low and high-frequency fluctuations combined in various ways. This inspires us to employ the matched filter to detect the desired signals out of noises. The matched filter is an optimal linear filter, made from a known signal template, to detect the template signal by maximizing its signal-to-noise ratio (SNR) from the unknown signals with stochastic noises [24]. For respiration monitoring, we can extract a single respiration cycle as the template for creating the matched filter and apply the matched filter on the received phase values to denoise it. The output of the matched filter will peak at where the template signal appears. After that, we can detect the peaks in the matched filter output and estimate the respiration rate.

For the matched filter, the respiration cycle template should be carefully selected for the following reasons. First, the shape of the template can affect the performance of the matched filter. Only when the template has the same shape with the desired signal can we achieve the optimal SNR. If the width or height of the template varies, the SNR of matched filter output will degrade. Second, respiration patterns are unique and diverse among different people [16], *e.g.*, the phase values of two persons' respiration in Fig. 9 show that their respiration cycles have different shapes. This means that the respiration cycle template should be unique for the monitored person to achieve high SNR of the matched filter output. Otherwise, if we make a unified template for all the users, the matched filter would not suit everyone. Therefore, the template should be exclusively extracted for the monitored person. We will discuss the effects of using the person's own template and other persons' template on the SNR in section IV.

To extract the respiration cycle template, we first pre-collect the pure respiration phase values of the monitored person in a static environment. The monitored person only needs to
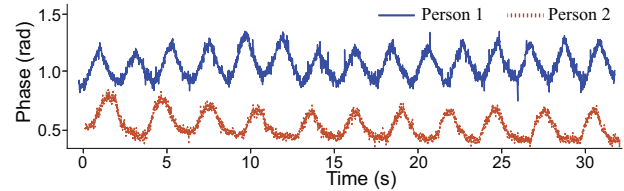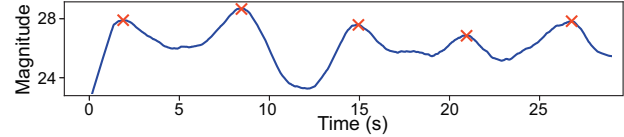
breathe normally for $2 - 3$ minutes with tens of respiration cycles obtained. This pre-collection phase is once for all, so it would not bring too much inconvenience to users. Thereafter, we extract the template from the collected respiration samples with a cycle-averaging method introduced as follows. First, the median filter is applied to smooth the raw phase values. Then, peak detection is performed on the negative of the phase values to extract the local minimum points. Based on the local minimum points, the whole phase series is segmented into several windows so that each window involves a single respiration cycle. Then, we obtain the average width and height of all the respiration cycles for later use. Next, we calculate the similarity between each pair of the respiration cycles based on the Euclidean distance. The respiration cycle with the highest pairwise similarity is selected as the template candidate. Finally, the template candidate is scaled according to the average width and height of all the respiration cycles for being the respiration cycle template $r_t(n)$. After that, the impulse response of the matched filter $h(k)$ is obtained from $r_t(n)$ as $h(k) = r_t(N - k - 1)$. N is the length of $r_t(n)$. In Fig. 10, we show the output after applying the matched filter on the phase values in Fig. 7(a). It presents 5 peaks, which exactly match the ground truth signals in Fig. 7(b).

C. Apnea detection

After removing the multipath effect, we first detect whether the respiration apnea appears. At first, we think that if there is no peak in the matched filter output for a while, we can regard that the apnea appears. However, for apnea detection, the matched filter does not work as we expect in the face of the fake respiration cycles caused by multipath signals. The reason is as follows. When the person is breathing, the matched filter can accurately extract the real respiration cycles mixed with fake cycles because real cycles have a higher correlation with the respiration cycle template compared with fake cycles. But when the person stops breathing, there is no real respiration cycle in the phase values. At this time, if multipath signals mimic a respiration-like wave, there would be a small peak in the matched filter output. For example, the phase values shown in Fig. 11(a) are collected from a person who stops breathing from $14 \ s$ to $24 \ s$ with people moving around. The
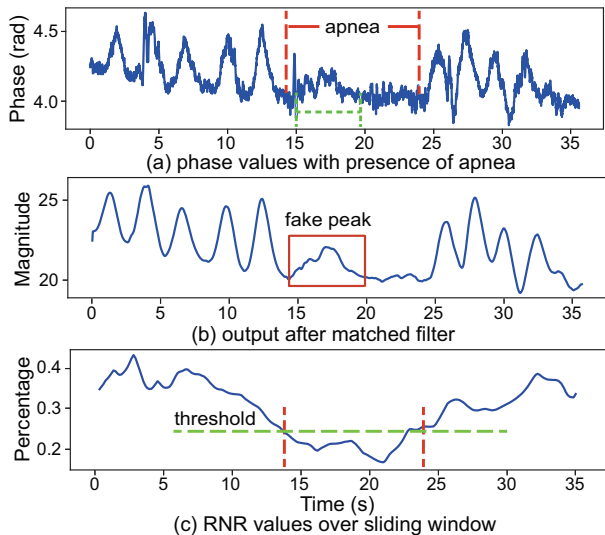
Fig. 11. Phase values, matched filter output and RNR of signals with apnea

multipath signals result in a respiration-like wave from $15\ s$ to $20\ s$. Although the wave has a smaller amplitude, it leads to a minor peak in the matched filter output, as shown in the red rectangular of Fig. 11(b). If the fake peak is not well identified, it can lead to the impression that the person is still breathing.

To differentiate the apnea from multipath signals, we investigate the original phase values in the frequency domain rather than using the matched filter output. When the monitored person is breathing, even though multipath signals bring noises to respiration signals, there are still dominant frequency components within the respiration rate range $(0.17\ Hz, 0.5\ Hz)$. If the person stops breathing, and only multipath signals are left, the frequency components resulting from moving behavior will take up a larger proportion compared with the components in the respiration rate range. Thus, we define a respiration-to-noise ratio (RNR) to identify the apnea. We first perform the fast fourier transformation (FFT) on the phase values. Then, in the whole spectrum $f(n)$, we get the maximum amplitude f_m in the respiration rate range and calculate the RNR by $RNR = f_m / \sum_{i=1}^{n} f(i)$.

RNR represents the percentage of the respiration components over all the frequency components. The RNR of pure multipath signals is lower than that of the respiration signals mixed with multipath signals. In Fig. 11(c), we show the RNRs for the phase values in Fig. 11(a). Here, RNR is calculated on $10\ s$-long sliding windows with 20 sample points as the interval. RNRs in $(14\ s, 24\ s)$, especially for the points around $21\ s$, are much smaller than other periods. To detect the decrease in RNRs for apnea detection, we calculate the RNR of the person's pre-collected respiration signals in the static environment, and the half of its RNR is set as the threshold σ. If the length of consecutive RNRs whose values are lower than σ exceeds $5\ s$, it is decided that the apnea appears, and the corresponding phase series will not be passed to perform respiration rate estimation. The length of $5\ s$ is chosen because it is the longest duration of normal respiration cycles [23].

D. Respiration rate estimation

To estimate the respiration rate, peak detection is applied to the matched filter output. The reason why we use peak detection instead of FFT is that the resolution of FFT is restricted by the length of time windows [10]. The resolution can be quite low if the real-time result is required. For instance, if we want a result every $20\ s$, the resolution in the frequency domain is $0.05\ Hz$ (i.e., $3\ bpm$), which may lead to inaccurate respiration rate. However, the peak detection approach suffers from the tiny fluctuations in the matched filter output. Because the peak detection algorithm would regard the small fluctuation point as a peak as long as its neighbor points are both below it. To avoid the adverse effect of fake peaks, previous methods set thresholds to discard the peaks which are too low or too closed to each other [5]. While the scale of the phase values will change from time to time. So, empirical thresholds may still incur missing or fake peaks. Therefore, to adapt to different scales automatically, we employ the automatic multi-scale peak detection (AMPD) [25]. AMPD frees us from choosing thresholds to detect the real peaks with the help of multi-scale technique. The detected peaks of the signals in Fig. 10 are shown with red crosses. Then, the respiration rate is estimated for each window as $rate = 60 / \frac{1}{n} \sum_{i}^{n-1} (p_{i+1} - p_i)$. $rate$ is in the unit of breath per minute (bpm). p_i is the timestamp of the peak. n is the total number of peaks.

IV. EVALUATION

In this section, we will introduce the experimental setup, evaluation metrics and the results in terms of different factors for apnea detection and respiration rate estimation.

A. Experimental setup

The experiments are done using commercial off-the-shelf RFID devices. The RFID reader is ImpinJ Speedway R420. The antenna is Laird E9208 antenna, and the tag is ImpinJ E41-C. The reader works in the $920-925\ MHz$ region and the reader mode is set as MaxThroughput. The reader is connected to a Dell Inspiron 7460 laptop with i7-7500U CPU and $8\ GB$ RAM. The RFID measurements are processed with Python 3.0. We did experiments in two different environments, as shown in Fig. 12. The antenna is put $1-2\ m$ away from the monitored person. The tag is attached to the person's chest. 10 volunteers act as the monitored person and surrounding people in turn. We do not assign specific routes for volunteers to move, so they can walk freely around the monitored person. The ground truth of the respiration signals is collected via a chest band equipped with a 3-axis accelerometer.

B. Evaluation metrics

To evaluate the performance of our system, the following metrics are used. First, the percentage of the missing apnea (MA) and false apnea (FA) over all the apnea cases are defined to illustrate the accuracy of apnea detection as $MA = \frac{\#missing\ apnea}{\#real\ apnea}$, $FA = \frac{\#false\ apnea}{\#no\ apnea}$.

Second, to evaluate the accuracy of respiration rate estimation, the mean absolute error (MAE) is defined as $MAE =$
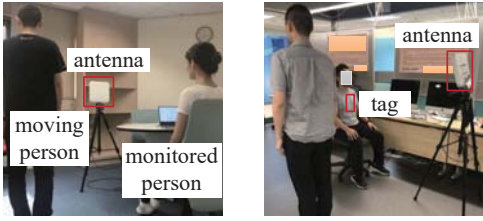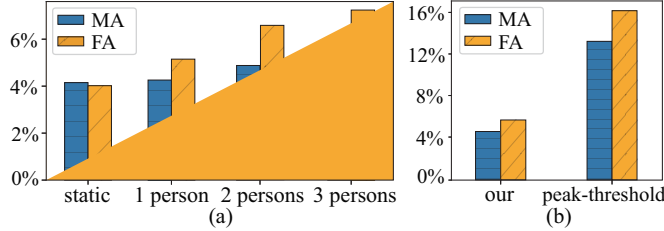
Fig. 12. Experimental settings in two environments

Fig. 13. Percentage of missing apnea (MA) and false apnea (FA) in the static environment, and with 1 person, 2 persons, 3 persons moving around
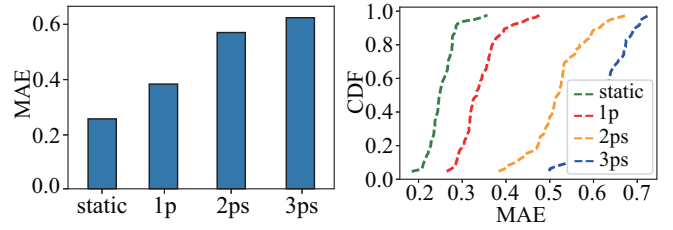

Fig. 14. MAE of respiration rate with different numbers of moving persons: no person (static), 1 person (1p), two persons (2ps) and three persons (3ps)

$\frac{1}{n}\sum_{i=1}^{n}|r_i - r_i'|$. r_i and r_i' are the estimated and real respiration rate, respectively. n is the number of samples.

C. Performance of apnea detection

1) Effect of number of moving people: We test our apnea detection approach in both static and dynamic environments with 0, 1, 2 and 3 persons moving around. We choose $1-3$ moving people because there would not be too many people walking around in indoor places like the living room and bedroom. Thus, 3 persons are enough for evaluation. During the experiment, volunteers who act as the monitored person are asked to simulate the apnea by holding their breath for $5-10\ s$. The results of MA and FA are shown in Fig. 13(a). Generally, MA and FA grow slightly with the increasing number of moving people, but they are both below 6% for all the cases. The average MA and FA with $1-3$ moving people are only $1\% - 2\%$ higher than those in the static environment. This indicates that our approach helps to enhance the robustness of apnea detection in dynamic environments. MA is slightly lower than FA because our approach is designed to decrease the cases of missing apnea. From the view of apnea diagnosis, patients can accept higher FA rather than higher MA, as higher MA may delay the detection of the apnea symptom.

2) Effect of the RNR indicator: Next, we compare the performance of our RNR-based approach with the previous peak-threshold approach to demonstrate the effectiveness of our approach on apnea detection in dynamic environments. The previous approach sets a threshold for the detected peaks of raw signals. If the detected peaks are below the threshold, they will treat the signals as apnea [5]. Here, the peak threshold is set as the mean of the phase values after applying the low-pass filter. The comparison results are given in Fig. 13(b). It shows that our approach outperforms the peak-threshold approach with an approximate 10% cutdown of MA and FA. This is because the fake peaks caused by the multipath signals from moving people would be regarded as breathing cycles in

the peak-threshold approach. Besides, the empirical threshold is not adaptive to the amplitude of peaks which can lead to more missing apnea. While our proposed RNR indicator can differentiate the real respiration signals from the multipath signals during the apnea period.

D. Performance of respiration rate estimation

1) Effect of matched filter: To show the effectiveness of the matched filter on respiration rate estimation, we first compare the MAE between the real and estimated respiration rates with and without applying the matched filter on the phase values. For the method without the matched filter, AMPD is directly applied to the phase values after denoising the signals with a median filter. For our method, the matched filter is first applied to denoise the phase values, then AMPD is employed for peak detection. The average MAE with the matched filter is $0.54\ bpm$. While the MAE without the matched filter is $3.06\ bpm$, which is around 5 times larger than that with the matched filter. This indicates that the matched filter can help to promote the accuracy of respiration rate estimation.

2) Effect of number of moving people: We further show the MAE results for different numbers of moving people in Fig. 14, including 0 (static), 1 (1p), 2 (2ps) and 3 persons (3ps). The distance between the person and antenna is set as $1.5\ m$. The average MAE goes up from $0.2\ bpm$ to $0.6\ bpm$ with more number of moving people because more people bring more multipath signals. The highest MAE, which happens with 3 moving persons, is still within $0.7\ bpm$. The CDF plot shows that most of MAEs are distributed within $0.6\ bpm$. We also compare the accuracy of respiration rate estimation of our system with existing systems in Table. I. Our system has a similar range of MAE to existing ones. Furthermore, [10] [12] are only designed for RM in static environments, while our system can also work in dynamic environments.

3) Effect of moving area: As mentioned in section II-B1, the moving area could affect $\vec{V}_{dm}$ and phase changes. Hence, we ask a volunteer to move inside and outside the $3\ dB$-area

TABLE I
COMPARISON OF RESPIRATION RATE ESTIMATION WITH EXISTING WORK

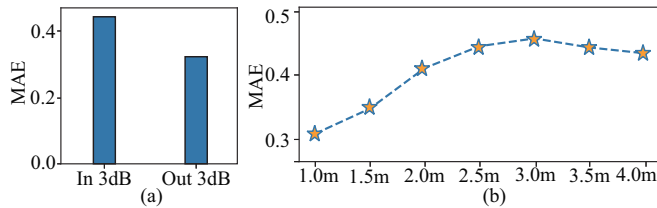|	[10]	[12]	our approach
MAE	0.5-1 bpm	0.3-0.5 bpm	0.3-0.6 bpm
Scenario	static	static	dynamic

Fig. 15. (a) MAEs for inside and outside 3 dB-area. (b) MAEs for different distances between antenna and person

Fig. 16. SNR and MAE with different persons' respiration templates

Fig. 17. MAE of other movements

to see the accuracy of respiration rate estimation, respectively. Since the inner 3 dB-area is a small area, so the experiment is done with only one moving person. The MAEs are shown in Fig. 15(a). When the person moves inside the 3 dB-area, the MAE is around 0.45 bpm, which is about 0.15 bpm higher than moving outside the 3 dB-area in average. Therefore, we can still achieve relatively high accuracy when the moving person is in the 3 dB-area of the antenna. In practice, since the 3 dB-area is quite a small region which mainly covers the LOS paths between the monitored person and antenna, people are less likely to move inside the 3 dB-area to disturb the respiration monitoring of the monitored person.

4) Effect of distance: Next, we see the effect of the distance between the antenna (A) and the monitored person (P) on respiration rate estimation. A longer distance between A and P also means a longer travelling distance of the signals, so the power of the signals backscattered to the antenna becomes less. Besides, the longer the distance between A and P, the larger the 3 dB-area will be. Then, there is a higher probability that the surrounding people would move inside the 3 dB-area. Hence, we change the distance from 1 m to 4 m with an interval of 0.5 m to see how the distance affects the accuracy of respiration rate estimation. Then, we ask one volunteer to move around the monitored person. The MAEs for different distances are shown in Fig. 15(b). The MAE increases with the distance going up from 1 m to 3 m, then it drops down slightly. The reason why MAE increases at the beginning is that the 3 dB-area becomes larger to allow the person to move inside the 3 dB-area, and the multipath signals bring more effects on the phase values. While, when the distance is larger than 3 m, the MAE drops because the multipath signals lose energy with a longer travelling distance. Furthermore, a longer distance between A and P also leads to fewer respiration LOS signals. Drawing the experience from current RFID-based RM studies, the antenna is usually put $1-2$ m away from the user.

5) Effect of respiration cycle template: In section III-B, we mentioned the performance of the matched filter can be affected by different templates. Here, we show the SNR of the matched filter output to see the effect. First, we collect the pure respiration phase values of 4 volunteers and extract 4 templates for them. Then, one volunteer (X) is selected as the monitored person (another 3 are denoted as A, B, C). We collect the phase values while X is breathing with 2 persons moving around. The 4 templates are made into 4 matched filters and use it to denoise X's phase values. The SNRs of the matched filter output and the MAEs of respiration rate using
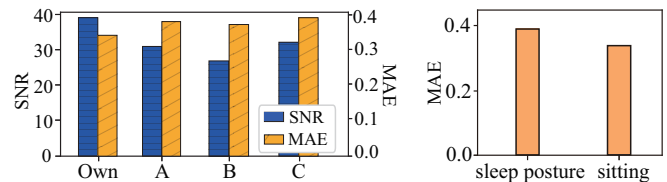
the matched filters with X's own and A's, B's, C's template are shown in Fig. 16, respectively. The SNR when using X's own template generated matched filter is the highest. Besides, the respiration rate MAE of using the person's own template is also slightly lower than those using other persons' templates, which infers the importance of choosing the proper template.

E. Performance of other movements

Apart from the walking movement, there are also other movements that could happen around the monitored person in daily RM scenarios. Here, we discuss some common cases. For example, for the couple in sleep, the movement of one person changing sleeping postures can bring multipath signals to the other person being monitored. For a person sitting beside the monitored person, the person's movements like stretching arms or turning around also incur multipath signals to the monitored person. Thus, we imitate the above scenarios and measure the respiration rate. The results are shown in Fig. 17, with MAE of changing sleeping postures as 0.39 bpm and MAE of sitting movements as 0.34 bpm. This shows that our approach also works well in these cases.

V. RELATED WORK

Our work is related to RF-based respiration monitoring and the multipath effect of wireless signals.

A. RF-based respiration monitoring

Recent advances in RF-based human sensing have witnessed their application in respiration monitoring. The motivation of RF-based sensing is that people can release themselves from wearing bulky sensors. Some systems use WiFi, UWB and FMCW radar for respiration monitoring by exploiting the multipath signals reflected by the chest [3], [8], [26]. The signal transmitter and receiver are put aside the person. The received signals change periodically with the expansion and contraction of chest while breathing. Some use RFID systems of which the tags are attached to the chest, and the backscattered LOS signals from the tags are used for respiration pattern extraction [10]–[12]. The advantage of RFID-based RM is that it is more scalable for the multi-person scenario, because the tags can help to differentiate the signals from different persons. While those studies that employ the multipath signals for respiration monitoring, *e.g.*, WiFi, suffer from the problem of precisely separating the respiration signals from different persons. That is why the expensive FMCW radar is used to further entangle the signals reflected by multiple persons [9]. In addition, the RFID tags are cheap, lightweight and easy to wear. Thus, it is convenient and cost-effective for users.

B. *Multipath effect of RF signals on respiration monitoring*

The multipath effect is a double-edged issue for RF-based human sensing. For one thing, multipath effect is the key advantage to take for non-intrusive sensing. Because the signals reflected by the human body contain the movement pattern. However, multipath effect is a hurdle when multiple persons are present. We need to separate the signals from different persons to capture the desired movements. For RM, people mainly monitor the respiration when the person is quasi-static, but we still face the multi-person issue. In [8] [9], FMCW radar is employed to extract the time of flight information of each signal path, so that the respiration signals of the desired person can be obtained. In [27], the authors try to remove the WiFi signals reflected by the surrounding moving people by widening the bandwidth via re-designing the protocol. RFID-based RM also faces the same multipath effect problem. But, current RFID-based respiration systems have the assumption that the environment is static, where no people move around the monitored person. However, the assumption limits the usage of the system in many practical scenarios. The system should be robust to report accurate respiration state in dynamic environments. Thus, our work aims to remove the multipath effect for RFID-based RM in dynamic environments and achieve robust respiration state estimation without modifying the off-the-shelf commercial RFID device and protocol.

VI. DISCUSSION

Our system, although trying to realized robust RFID-based RM in dynamic environments, still has some limitations. First, people's respiration pattern could change over time. Therefore, the template should be updated from time to time to guarantee accuracy. Second, for sleep apnea detection, we only detect the sudden stop breathing. However, there are also hypopnea and obstructive apnea, which need further studies to detect them.

VII. CONCLUSION

In this work, we push forward the application of RFID-based RM. Previous systems have realized RM in the static environment. While in dynamic environments, the moving people bring multipath signals which distort the respiration pattern in the RFID phase values. Therefore, we propose to enhance the robustness of RFID-based RM in dynamic environments. The effect of the multipath signals is eliminated by employing the matched filter to detect the desired respiration cycles from the noisy phase series. The respiration rate is then obtained by counting the peaks in the matched filter output. To identify the apnea out of the multipath signals which could mimic the pattern of breathing cycles, we draw on the dominance of respiration components in the frequency domain to avoid the missing detection of apnea. The evaluation results show that our approach can promote the accuracy of respiration monitoring in dynamic environments.

VIII. ACKNOWLEDGEMENT

REFERENCES

[1] "Sleep apnea," https://www.nhlbi.nih.gov/health-topics/sleep-apnea, accessed: 2019-09-01.
[2] "Chronic respiratory diseases," https://www.who.int/health-topics/chronic-respiratory-diseases, accessed: 2019-09-01.
[3] X. Liu, J. Cao, S. Tang, and J. Wen, "Wi-sleep: Contactless sleep monitoring via wifi signals," in *Proc. IEEE RTSS*, 2014.
[4] H. Wang, D. Zhang, J. Ma, Y. Wang, Y. Wang, D. Wu, and T. Gu, "Human respiration detection with commodity wifi devices: do user location and body orientation matter?" in *Proc. ACM Ubicomp*, 2016.
[5] J. Liu, Y. Wang, Y. Chen, J. Yang, X. Chen, and J. Cheng, "Tracking vital signs during sleep leveraging off-the-shelf wifi," in *Proc. ACM MobiHoc*, 2015.
[6] T. Rahman, A. T. Adams, R. V. Ravichandran, M. Zhang, S. N. Patel, J. A. Kientz, and T. Choudhury, "Dopplesleep: A contactless unobtrusive sleep sensing system using short-range doppler radar," in *Proc. ACM Ubicomp*, 2015, pp. 39–50.
[7] X. Wang, C. Yang, and S. Mao, "Phasebeat: Exploiting csi phase data for vital sign monitoring with commodity wifi devices," in *Proc. IEEE ICDCS*, 2017.
[8] F. Adib, H. Mao, Z. Kabelac, D. Katabi, and R. C. Miller, "Smart homes that monitor breathing and heart rate," in *Proc. ACM CHI*, 2015.
[9] S. Yue, H. He, H. Wang, H. Rahul, and D. Katabi, "Extracting multi-person respiration from entangled rf signals," *Proc. ACM IMWUT*, 2018.
[10] Y. Hou, Y. Wang, and Y. Zheng, "Tagbreathe: Monitor breathing with commodity rfid systems," in *Proc. IEEE ICDCS*, 2017.
[11] C. Yang, X. Wang, and S. Mao, "Autotag: Recurrent variational autoencoder for unsupervised apnea detection with rfid tags," in *Proc. IEEE GLOBECOM*, 2018.
[12] R. Zhao, D. Wang, Q. Zhang, H. Chen, and A. Huang, "Crh: A contactless respiration and heartbeat monitoring system with cots rfid tags," in *Proc. IEEE SECON*, 2018.
[13] C. Wang, L. Xie, W. Wang, Y. Chen, Y. Bu, and S. Lu, "Rf-ecg: Heart rate variability assessment based on cots rfid tag array," in *Proc. ACM IMWUT*, 2018.
[14] Y. Wang and Y. Zheng, "Modeling rfid signal reflection for contact-free activity recognition," in *Proc. ACM IMWUT*, 2018.
[15] X. Fan, W. Gong, and J. Liu, "Tagfree activity identification with rfids," in *Proc. ACM IMWUT*, 2018.
[16] G. Benchetrit, "Breathing pattern in humans: diversity and individuality," *Respiration physiology*, vol. 122, no. 2-3, pp. 123–129, 2000.
[17] P. V. Nikitin, R. Martinez, S. Ramamurthy, H. Leland, G. Spiess, and K. Rao, "Phase based spatial identification of uhf rfid tags," in *Proc. IEEE RFID*, 2010.
[18] X. Lai, Z. Cai, Z. Xie, and H. Zhu, "A novel displacement and tilt detection method using passive uhf rfid technology," *Sensors*, vol. 18, no. 5, p. 1644, 2018.
[19] "Rfid antennas," https://media.digikey.com/pdf/Data-Sheets/Laird-Technologies/RFID-Antennas.pdf, accessed: 2019-09-01.
[20] D. M. Dobkin, *The RF in RFID: uhf RFID in practice*. Newnes, 2012.
[21] W. Wang, A. X. Liu, and M. Shahzad, "Gait recognition using wifi signals," in *Proc. ACM Ubicomp*, 2016.
[22] "Human walking speed," https://en.wikipedia.org/wiki/Walking, accessed: 2019-09-01.
[23] "Respiration rate," https://en.wikipedia.org/wiki/Respiratory-rate, accessed: 2019-09-01.
[24] R. G. Lyons, *Understanding digital signal processing, 3/E.* Pearson Education India, 2004.
[25] F. Scholkmann, J. Boss, and M. Wolf, "An efficient algorithm for automatic peak detection in noisy periodic and quasi-periodic signals," *Algorithms*, vol. 5, no. 4, pp. 588–603, 2012.
[26] Y. Yang, J. Cao, X. Liu, and X. Liu, "Multi-breath: Separate respiration monitoring for multiple persons with uwb radar," in *Prof. IEEE COMPSAC*, 2019.
[27] S. Shi, Y. Xie, M. Li, A. X. Liu, and J. Zhao, "Synthesizing wider wifi bandwidth for respiration rate monitoring in dynamic environments," in *Proc. IEEE INFOCOM*, 2019.